ACES Asian Chemical Editorial Society

doi.org/10.1002/asia.202500140

CHEMISTRY
AN ASIAN JOURNAL
Research Article

www.chemasianj.org

Isothermal Dehydrogenation of Ammonia Borane: Insights into BNH Polymers and Challenges in Regeneration

Carlos A. Castilla-Martinez,*[a] Philippe Gaveau,[b] Mona Semsarilar,[a] Bruno Alonso,[b] and Umit B. Demirci*[a]

In this study, the BNH polymers produced by ammonia borane (AB) thermolysis under isothermal conditions were investigated. Polyaminoborane (PAB) and diammoniate of diborane (DADB) form upon releasing the first equivalent of H_2 at 85 °C, followed by the formation of cross-linked polyborazylene (PB) at 140 °C. Polyiminoborane (PIB) was not detected under these conditions. The characterization of these BNH polymers, relied on solid-state techniques including IR, Raman, XPS, and ^{11}B MAS NMR. These methods revealed the chemical diversity and structural complexity of PAB and PB, highlighting the presence of different boron environments. The stability of the BNH polymers was also investigated over time and under different atmospheres. Over six months, both PAB and PB exhibited increased polymerization, and PAB showed an interesting ability to adsorb carbon dioxide. Efforts to regenerate AB from PAB and PB through hydrogenation and ammonia-based methods were conducted. The experiments showed that the BNH polymers break into smaller molecules, showing partial rehydrogenation of –NH and –BH groups in some cases, but with limited efficiency. Higher temperatures and hydrogen pressure modified decomposition pathways, though complete regeneration remains challenging. This study offers new insights into the chemical structure of BNH polymers and their potential use as hydrogen storage materials.

Introduction

One of the most promising alternatives to fossil fuels is hydrogen (H_2). Current technologies to store hydrogen primarily rely on pressurized or cryogenic tanks.[1] Hydrogen stored in materials is an attractive option, as it offers higher volumetric energy density, enhanced safety, and potential for reversible storage.[2] Various materials have been proposed for this purpose, including porous materials (e.g. carbon-based materials, metal organic frameworks, zeolites), liquid hydrogen carriers (e.g. toluene, dibenzyltoluene, ammonia) and hydrides (e.g. metal hydrides, complex hydrides and, chemical hydrides). These materials pose different challenges: for instance, the storage conditions for porous materials (at −196 °C), the overall efficiency of the system, the high dehydrogenation temperature for most of metal hydrides and the low storage capacity of interstitial hydrides.[3] Ammonia borane (AB, NH_3BH_3) is one material that overcomes most of these disadvantages and stands out for several reasons. It is stable under ambient conditions and inert atmosphere, exhibits a high gravimetric (19.6 wt. % H_2) and volumetric hydrogen density (146 g_{H2} L^{-1}), and can release H_2 via thermolysis, hydrolysis, or alcoholysis.[4] The thermolysis of AB is particularly attractive, as it can release approximately 13 wt. % H_2 when heated to 200 °C, which represents 2 equivalents of H_2 out of the 3 that it carries. Despite these advantages, several challenges associated with thermolysis have hindered its scalability and application in hydrogen storage technologies. These challenges include: i) high dehydrogenation temperatures (> 100 °C); ii) the release of undesirable gaseous byproducts (e.g. ammonia NH_3 and borazine $B_3H_6N_3$); iii) formation of BNH polymers with complex composition; and iv) the irreversibility of the reaction. While significant progress has been made in addressing challenges i) and ii) – for example, by incorporating additives, nanosizing AB, or chemically modifying it to lower the dehydrogenation temperature and suppress byproducts, – issues iii) and iv) have been relatively underexplored.

The thermolysis of AB can be conducted using two distinct approaches: dynamic conditions (e.g. thermogravimetric analysis) or static conditions (e.g. isothermal treatment). AB undergoes different dehydrogenation pathways depending on the conditions of the chosen approach. The dynamic dehydrogenation of AB has been summarized in three key steps.[5–7] Between 100 and 130 °C, AB releases the first equivalent of H_2, forming polyaminoborane (PAB, $(H_2N–BH_2)_n$). In the 130–200 °C range, the second equivalent of H_2 is released, producing polyiminoborane (PIB, $(HN{=}BH)_n$) and polyborazylene (PB, $(B_3H_4N_3)$), a cyclic BNH polymer. Above 200 °C, PB is present upon the formation of hexagonal boron nitride (h-BN) at higher temperatures (> 1200 °C). In reality, this is not a step-wise process. Once AB starts to release H_2, a solid residue comprising

[a] Dr. C. A. Castilla-Martinez, Dr. M. Semsarilar, Prof. U. B. Demirci
Institut Européen des Membranes, IEM – UMR 5635 (Univ Montpellier, ENSCM, CNRS), 34095 Montpellier, France
E-mail: carlos.castilla-martinez@umontpellier.fr
ccastilla90@gmail.com
umit.demirci@umontpellier.fr

[b] Dr. P. Gaveau, Dr. B. Alonso
ICGM, Université de Montpellier, CNRS, ENSCM, 34293, Montpellier, cedex 5, France

Supporting information for this article is available on the WWW under https://doi.org/10.1002/asia.202500140

a mixture of BNH polymers forms.[8–10] This residue remains poorly characterized. Compared to the dynamic approach, AB can be dehydrogenated at lower temperatures under isothermal conditions (e.g. 75 °C), but with a slower hydrogen release.[11]

The regeneration of dehydrogenated AB products is another major challenge. Two primary approaches have been reported in the literature: digestion-based regeneration and hydrazine-based regeneration. The digestion-based approach has been explored in some studies. In one of them, the BNH polymers formed after AB thermolysis were directly digested in HCl for 16 h.[12] This produces BCl_3 and NH_4Cl; the former is converted into diborane through a reaction with a borane complex, while the latter is decomposed into NH_3. Diborane and NH_3 are then combined to regenerate AB. Another study focused on PB rather than the BNH polymer mixture.[13] PB was digested with benzenedithiol for 12 h, forming a B–S bonded complex, which was subsequently reduced using a tin-based hydride to regenerate AB with a 67% yield. The second approach is the hydrazine-based one, which also uses PB as the starting material, and it involves the reaction of this compound with hydrazine in ammonia.[14] This method achieves a regeneration yield of 92% for AB and 8% for hydrazine borane. While these methods have demonstrated success in regenerating AB, they also present notable drawbacks. The digestion-based approach is multi-step, requiring a variety of chemicals, making it both complex and costly. Meanwhile, the hydrazine-based method relies on "pure" PB and suffers from low energy efficiency.[15]

To develop a reversible hydrogen storage system based on AB, a deeper understanding of the structure and properties of single BNH polymers formed during thermolysis is essential (i.e. PAB, PIB, and PB). Furthermore, new, cost-effective regeneration pathways must be explored. This study aims to isolate and characterize each one of the three main BNH polymers –PAB, PIB, and PB– formed during AB thermolysis. Additionally, we investigate an alternative regeneration strategy inspired by hydrocracking processes, which uses a catalyst under H_2 pressure and elevated temperatures to break hydrocarbons. We hypothesized that this approach could fragment the BNH polymers into smaller molecules, which could then be hydrogenated to regenerate AB. The results of our investigation are presented herein.

Results and Discussion

Preliminary Observations

Recrystallized AB was analyzed by ^1H and ^{11}B solution Nuclear Magnetic Resonance (NMR) (Figure S1). The ^{11}B NMR spectrum of AB shows a single quadruplet centered at 24 ppm, characteristic of the NBH_3 environment of the molecule.[16] The ^1H NMR spectrum displays different signals: the characteristic quadruplet centered at 1.4 ppm due to the BH_3 environment, a triplet associated to the NH_3 moiety at 3.6 ppm, the signals corresponding to the residual solvent acetonitrile CH_3CN at 1.98 ppm, the H_2O present in the deuterated solvent at 2.2 ppm, and a small signal present at 4.6 ppm attributed to H_2 (dissolved and coming from AB hydrolysis).

Through an isothermal heat treatment of AB, two distinct BNH polymers were obtained. The first, PAB, was obtained following a heat treatment at 85 °C. The second, PB, was synthesized through a two-step process involving heat treatments at 85 °C and 140 °C. However, the presence of PIB was not detected, even though different conditions were tested. For example, at an intermediate temperature of 110 °C, the IR spectrum of the compound is a mixture of the spectra of PAB and PB (Figure S2). The absence of PIB can be explained by different reasons. Li *et al.*[17] conducted a theoretical study showing that the dehydrogenation of AB leads to the formation of PAB and $H(NH_2BH_2)_nH$ oligomers. These oligomers face significant energy barriers to further dehydrogenation. For instance, the oligomer with $n=3$ exhibits a dehydrogenation barrier of 49.4 kcal mol^{-1}, via head-to-tail hydrogen transfer, which results in cyclotriborazine (CTB) formation. A more favorable pathway, with an energy barrier of 40 ± 3 kcal mol^{-1}, involves hydrogen transfer between terminal and neighboring atoms (e.g. from $NH_3BH_2NH_2BH_2NH_2BH_3$ to $NH_2{=}BHNH_2BH_2NH_2BH_3$ or $NH_3BH_2NH_2BH_2NH{=}BH_2$). In the resulting unsatured oligomer, one of the B–N bonds is cleaved (28 kcal mol^{-1}), leading to CTB formation. Another possible reaction involves the scission of larger oligomers into shorter species with the release of the unstable aminoborane NH_2BH_2 (e.g. $NH_3BH_2(NH_2BH_2)_nNH_2BH_3$ into $NH_3(NH_2BH_2)_nBH_3 + NH_2BH_2$). This is a first indication that the formation of CTB is favored over that of PIB. Lory and Porter detected the highly reactive iminoborane (HNBH) in gaseous state via IR spectroscopy, via photodecomposition of AB.[18] It has been suggested that HNBH can undergo two competing reactions:[6] trimerization to form borazine or dehydrogenation to yield NH_2BH_2. This suggests again that the formation of cyclic compounds or that of PAB is preferred over the formation of PIB. Miranda and Ceder predicted the favorable thermodynamic formation of PIB from AB at −273 °C through density functional theory calculations.[19] Their model indicated that PIB is more stable than borazine. On the one hand, different studies show that the dehydrogenation pathway of AB does not lead to the formation of PIB, as it rather transforms into PAB and cyclic compounds; on the other hand, PIB was predicted to form, but at subzero conditions. In other words, the isolation and identification of PIB have not yet been experimentally proven under ambient conditions, nor in the liquid or solid state. Jeong *et al.* proposed that PIB could form directly from AB confined within a metal organic framework, the MOF-5.[20] According to their study, the narrow pores of MOF-5 suppress borazine formation, favoring the direct formation of PIB. Nevertheless, the evidence provided is insufficient to conclusively confirm the formation of PIB. Kobayashi *et al.* investigated the dehydrogenation of bulk AB under vacuum across different conditions and performed detailed Magic Angle Spinning (MAS) NMR analyses of the resulting products.[21] They did not detect PIB formation and concluded that PB forms via the direct dehydrocyclization of PAB. This conclusion is supported by other studies that have considered polyiminoboranes as elusive polymers.[22,23] In summary, while

the term "*polyiminoborane*" is often used in AB dehydrogenation research to describe a linear polymer with the formula $(HN{=}BH)_n$, but experimental evidence confirming the formation of such structures is lacking. Current data suggest that AB primarily forms PAB, which subsequently transforms directly into PB, without forming PIB. This aligns with the findings of the present study, where PIB was not produced, and only PAB and PB were obtained.

As previously mentioned, the characterization of BNH polymers remains challenging. Conventional polymer characterizations methods are impractical – if not impossible – due to the insolubility of these compounds. In this study, multiple solvents were tested in an attempt to dissolve PAB and PB, but all attempts failed. As a result, only solid-state analysis techniques were employed, as discussed in the following sections.

Elemental Analysis

ICP-MS and CHN elemental analysis were conducted to determine the elemental composition of the BNH polymers. The theoretical mass percentages for PAB are 37.5 wt.% B, 48.6 wt.% N, and 13.9 wt.% H, based on the monomer unit formula $(B_{1.00}N_{1.00}H_{4.00})_n$ (B/N = 1). The experimentally obtained values were 37.8 wt.% B, 43.6 wt.% N, and 12.5 wt.% H, corresponding to an empirical formula $(B_{1.00}N_{0.89}H_{3.50})_n$ (B/N = 1.13). Similarly, the theoretical mass percentages for PB are 41.3 wt.% B, 53.5 wt.% N, and 5.1 wt.% H, assuming the monomer formula $(B_{3.00}N_{3.00}H_{4.00})_n$ (B/N = 1). Experimentally, the composition was determined to be 41.8 wt.% B, 45.7 wt.% N, and 4.5 wt.% H, yielding an empirical formula $(B_{3.00}N_{2.50}H_{3.57})_n$ (B/N = 1.2). Pressure measurements were taken before and after the isothermal heat treatment used to synthesize the BNH polymers. The difference in pressure between the start and end of the experiments was used to calculate the equivalents of gases released, assuming ideal gas behavior. Theoretically, the dehydrogenation process to form PAB and PB is expected to release 1 and 2 equivalents of H_2, respectively. Experimentally, the amounts of gas released during the synthesis of PAB and PB were 1.14 and 2.16 equivalents, respectively (Supporting Information, Experimental Section). It is likely that NH_3 was released alongside H_2 during the synthesis of the BNH polymers, which would explain the discrepancy between the theoretical and experimental B/N ratios. Otherwise, the theoretical and experimental compositions have a good match.

Vibrational Spectroscopy

AB and the BNH polymers were analyzed using IR and Raman spectroscopy (Fig 1). On the AB IR spectrum, the stretching vibrational modes of N–H and B–H appear between 3100–3450 cm^{-1} and 2050–2550 cm^{-1}, respectively, while the bending vibrational modes of N–H and B–H are observed at 1300–1700 cm^{-1} and 930–1300 cm^{-1}, respectively.[24] Two bands located at 650–880 cm^{-1} are attributed to the B–N stretching vibrational mode of the molecule. The IR spectrum of PAB closely resembles that of AB, with some notable differences. The N–H and B–H bending modes, as well as the B–N stretching mode, are broadened and slightly shifted, consistent with the polymerization of AB. The N–H bending mode redshifted, while the B–N stretching mode blueshifted. This spectrum aligns with previously reported data for crystalline PAB.[25,26] In contrast, the IR spectrum of PB shows more pronounced changes. The N–H and B–H stretching modes merge into a single, sharper band, resembling PB synthesized by the direct polymerization of borazine,[27] and both have blueshifted. These changes are attributed to cyclization during polymerization. Additionally, a broad band centered at 1400 cm^{-1}, characteristic of the B–N stretching mode in cyclic structures appears, while the B–N bending mode is observed at 890 cm^{-1}.

The Raman spectrum of AB corresponds well with previously reported data (Figure 1b).[28] The bands at 3250 and 3316 cm^{-1} correspond to the symmetric and asymmetric N–H stretching modes, respectively; the bands at 2282 and 2376 cm^{-1} to the symmetric and asymmetric B–H stretching modes, respectively; the band at 1598 cm^{-1} to the NH_3 bending mode; the bands at 1157 and 1190 cm^{-1} to the BH_3 bending

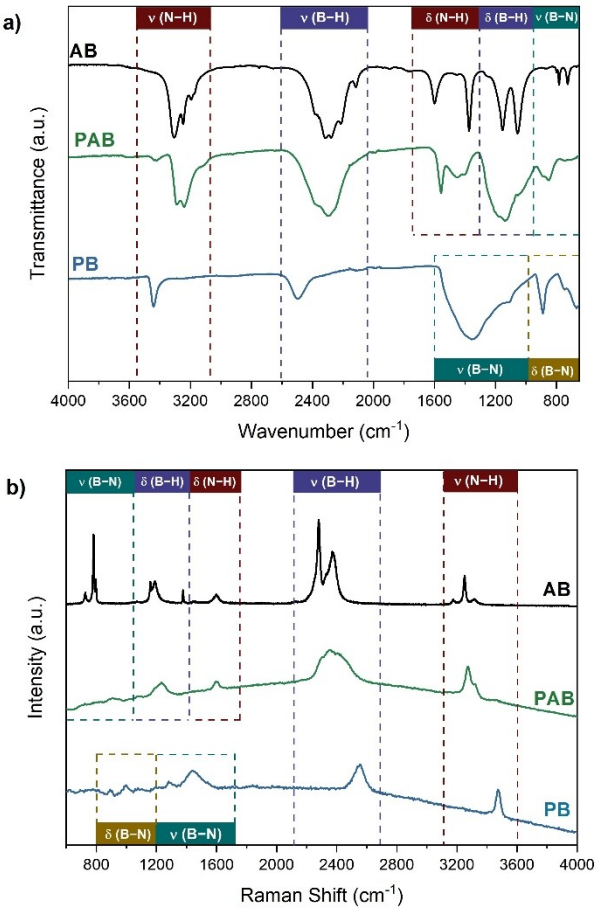

Figure 1. a) IR spectra; and b) Raman spectra of AB, PAB and PB. The vibrational modes have been assigned and indicated in the rectangles.

vibrations; the band centered at 782 cm^{-1} to the B–N stretching mode; and the band at 730 cm^{-1} to the NBH rocking mode. Similar to the IR results, the Raman spectrum of PAB exhibits broader bands, which can be assigned analogously to those of AB. Notably, the bands at 1598 and 1233 cm^{-1} are now attributed to the bending vibrations of NH_2 and BH_2 groups, respectively.[29] The Raman spectrum of PB is comparable to that of borazine.[30] The N–H and B–H stretching bands shift to higher frequencies, reflecting the altered environment in the cyclic or cross-linked structure. The band centered at 1440 cm^{-1} corresponds to the asymmetric B–N stretching mode, while the bands between 900 and 1100 cm^{-1} are assigned to the in-plane and out-of-plane B–H bending modes of the cyclic ring.

Crystal Structure

AB, PAB and PB were analyzed by XRD (Figure S3). AB exhibits a crystalline structure, with a body-centered tetragonal unit cell with an *I*4 *mm* space group at room temperature.[31] The XRD pattern of PAB displays an intense peak at 23° ($d_{spacing}$ = 3.81 Å) and a smaller peak at 41° ($d_{spacing}$ = 2.19 Å), suggesting the formation of semicrystalline linear PAB. However, the possibility of cyclic, branched or oligomeric structures cannot be excluded at this point. The $d_{spacing}$ of the PAB obtained in this study is slightly higher than those reported by He *et al.* ($d_{spacing}$ = 3.78 Å) and Staubitz *et al.* ($d_{spacing}$ = 3.6 Å) for PAB produced via dehydrogenation of AB using FeB and iridium-based catalysts, respectively.[25,26] The observed difference in $d_{spacing}$ indicates a slight structural variation in the PAB obtained in this work, perhaps a lower degree of crystallinity, likely due to the lack of a catalyst for dehydrogenation. PB presents an amorphous structure, with two broad bands centered at 26° and 42°, which are associated to the (002) and (100) reflection planes.[32] The former is associated with the interlayer spacing in graphite-like domains, and the later with the in-plane lattice parameter of six-membered rings.

X-ray Photoelectron Spectroscopy

AB, PAB, and PB were analyzed using XPS (Figure 2). The signals were assigned and interpreted based on the NIST database, and on the work of Papp and collaborators.[33–35] The B 1s spectrum of AB was deconvoluted in three signals centered at 189.3, 190.6 and 192.4 eV. The signal at 189.3 eV corresponds to NH_3BH_3, while the one at 190.6 eV is attributed to a BNH compound formed from the decomposition of AB. In a previous

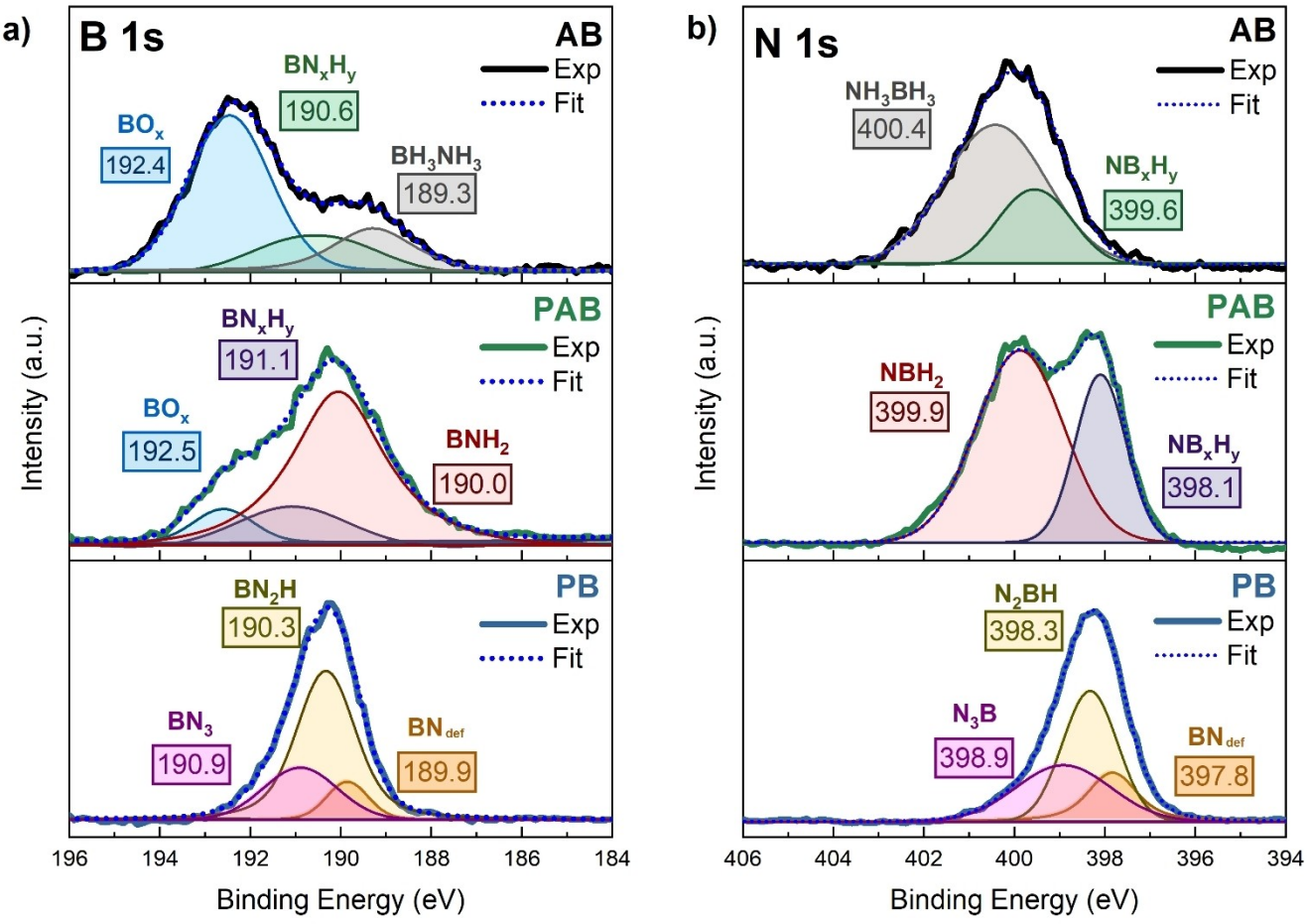

Figure 2. XP spectra of AB, PAB, and PB for a) B 1s and b) N 1s. The spectra were deconvoluted and the binding energies in eV are indicated in the colored rectangles.

study, we observed that X-ray irradiation during analysis can cause dehydrogenation of borane compounds, producing similar BNH species.[36] At 192.4 eV, an intense signal associated to BO_x is observed. The signal at 192.4 eV is associated with BO_x and represents 61.3% of the total area of the spectrum, highlighting the susceptibility of AB to hydrolysis under ambient conditions. This result is likely because the sample was prepared in air before being introduced into the XPS apparatus. Additionally, the area ratio between the decomposition product (BNH) and AB signals is 1.1, indicating that AB readily decomposes under X-ray irradiation. The N 1s spectrum of AB shows two signals: one at 400.4 eV corresponding to NH_3BH_3 and another at 399.6 eV, corresponding to the BNH decomposition product. In the B 1s spectrum of PAB, three signals are also observed. The BO_x signal is present at 192.5 eV, but its intensity is significantly reduced to 9.6%, indicating that PAB is more resistant to be hydrolyzed compared to AB. Similarly, the BNH decomposition product signal is detected at 191.1 eV, but the area ratio between this and the PAB signal (at 190.0 eV) is only 0.26. This lower ratio reflects the dehydrogenated state of PAB, which enhances its stability under X-ray irradiation. In the N 1s spectrum of PAB, two signals are observed: one at 399.9 eV, corresponding to PAB, and another at 398.1 eV, attributed to the BNH decomposition product.

The B 1s spectrum of PB exhibits notable differences. The BO_x signal is absent, suggesting that PB is resistant to oxidation. Additionally, the BNH decomposition product signal is not detected. The spectrum shows three main signals: 189.9 eV, attributed to an H_2B–N environment similar to PAB; 190.3 eV, corresponding to HB–N_2, as in polyborazylene; and 190.9 eV, associated with BN_3 environments, indicative of a cross-linked PB structure. This interpretation is consistent with the insolubility of PB, in contrast to reports of soluble PB.[37] The B/N atomic ratio of PB obtained by XPS is 1.20, closely matching the ratio of 1.18 determined by elemental analysis, indicating that the surface composition of PB is similar to its bulk composition.

The N 1s spectrum of PB reflects the same bonding environments as the B 1s spectrum. The binding energies of the three compounds confirm a trend: as the dehydrogenation of AB proceeds, the B binding energy increases while the N binding energy decreases. For example, the B 1s binding energies are 189.3 eV for AB, 190.0 eV for PAB, and 190.9 eV for PB. Conversely, the N 1s binding energies are 400.4 eV for AB, 399.9 eV for PAB, and 398.9 eV for PB. This trend can be correlated with the variation in the B–N bond length. The B–N bond length in AB has been calculated as 1.682 ± 0.058 Å.[38] In linear PAB with 2–16 monomer units, the B–N bond length ranges from 1.569 to 1.591 Å.[39] Borazine and hexagonal boron nitride exhibit shorter B–N bond lengths of 1.4355 Å and 1.47 Å, respectively.[40,41] As AB undergoes dehydrogenation, the B and N atoms form a double bond, and it becomes shorter and more stable. The increased attraction of nitrogen's lone-pair electrons to boron raises the B binding energy, while the reduced electron density on nitrogen lowers its binding energy. The signals at 189.9 eV (B 1s) and 397.8 eV (N 1s) are associated to defective and disordered boron nitride.[34] This could be explained by the formation of PB with a high degree of cross-linking during the XPS analysis.

Solid-State ^{11}B NMR

PAB was analyzed by ^{11}B MAS NMR (Figure 3a), and the chemical environments were assigned with the aid of complementary ^{11}B multiple quantum (MQ) MAS NMR analysis (Figure 3b). The six resonances observed between 0 and −40 ppm and at negative chemical shifts are characteristic of tetracoordinated boron atoms. They present weak quadrupolar interactions (ellipsoidal cross-peaks very close to the diagonal in Figure 3b). The signal at −37 ppm is assigned to a BH_4 environment, while the signal at −14 ppm corresponds to a N_2BH_2 environment, associated with the diammoniate of diborane (DADB, $[(NH_3)_2BH_2]^+[BH_4]^-$).[21,42] DADB is a reactive ionic dimer formed during AB thermolysis.[43,44] It is likely that the −14 ppm signal also reflects contributions from the polymeric chains of PAB.[42,45]

The signal at −23 and −27 ppm are assigned to a NBH_3 environment, likely originating from the termini of polymeric PAB chains and a mobile phase of AB.[46–48] Another signal, detected at −7 ppm is attributed to N_3BH environments, likely resulting from branched PAB structures, as well as the signal present at 1 ppm, assigned to BN_4 environments.[21,49] In the positive chemical shift region, typical of tricoordinated boron atoms, a signal between 15 and 30 ppm was observed, indicating that heating to 85 °C initiates the formation of BNH compounds with sp^2 hybridization (e.g. PB).

The PB spectrum exhibits two massifs of overlapped resonances (Figure 3c). The first, with a maximum peak intensity centered at −15 ppm, indicates the presence of residual PAB within the compound. The main massif appears between 10 and 40 ppm, and it is composed of tricoordinated boron atoms. ^{11}B MQ MAS analysis allows to obtain the NMR parameters of each boron site,[50] such as the isotropic chemical shift δ_{iso}, the quadrupolar coupling constant C_Q, and the asymmetry parameter η_Q, which gives valuable information about the chemical environment of the B atoms. The ^{11}B MQ MAS NMR spectrum of PB is shown in Figure 3d. The signals of this second massif present stronger quadrupolar interactions in comparison to those of PAB. Their parameters were obtained by spectrum fitting (see Supporting Information and Figure S4) and presented in Table 1. In the literature, these signals have been typically assigned to HB═N_2 and N_2B═N environments, likely of a PB structure.[45,51–54] We have noticed that the MQ MAS signals belonging to PB present an "atypical" shape. However, this

Table 1. NMR parameters of ^{11}B PB signals.

δ_{iso} (ppm)	C_Q (kHz)	η_Q	B environment
26.7	2700	0.29	BN_3
28.5	2850	0.20	BN_3
31.5	3100	0.35	NBH_2
35.6	3360	0.37	NBH_2

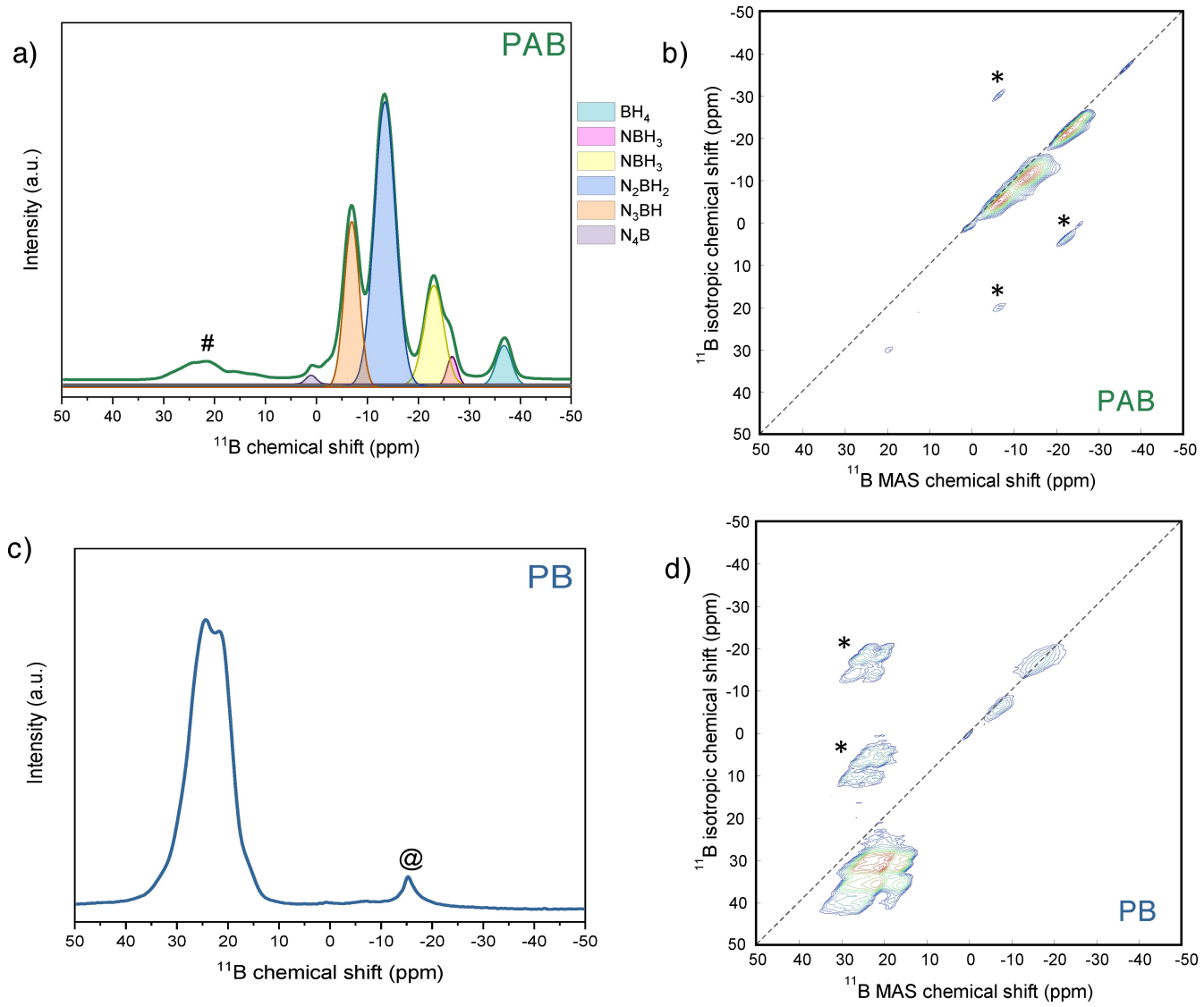

Figure 3. a) ^{11}B MAS and HR MAS NMR spectra of PAB together with the respective fitted moles. The chemical environments are indicated by colors. b) MQ MAS NMR spectrum of PAB; c) ^{11}B MAS and d) MQ MAS NMR spectra of PB. The raw 2D spectra have been sheared to present the isotropic chemical shift axis in F1. The # represent the resonance of PB in PAB, the @ the resonance of PAB in PB, and the * corresponds to spinning sidebands cross-peaks.

phenomenon has been also observed in different publications.[21,50,52,55]

To gain further insight into the structure of this BNH polymer and the chemical environment of these signals, ^{11}B{^{1}H} Cross Polarization (CP) MAS NMR with variable contact time (τ_c) was performed. CP MAS NMR allows the polarization transfer ^{1}H→^{11}B via the ^{1}H–^{11}B dipolar interaction. Different ^{11}B{^{1}H} CP MAS spectra of PB were obtained by varying τ_c (Figure S5). They were fitted using the NMR parameters of Table 1. Figure 4 presents the variations in intensity of the four signals as a function of τ_c. These curves depend on different factors, including ^{1}H–^{11}B dipolar interaction and relaxation times ($T_{1\rho}$^{1}H) notably). Curves presenting faster initial rates would correspond to environments with stronger dipolar interactions, indicating here shorter H···B distances. In the case of PB, the boron environments observed at δ_{iso} = 35.6 and 31.5 ppm are likely directly bonded to hydrogen atoms, forming N_2BH units. A similar trend was observed when investigating PB as a preceramic precursor to boron nitride, with comparable findings indicating that the N_2BH sites exhibited faster rates compared to the BN_3 sites.[52] According to the literature, BN_3 environments have been reported at approximately 27 ppm in poly(aminoborazine).[52] Given that PB exhibits two boron environments at 26.7 and 28.5 ppm, and that these environments are characterized by longer H···B distances, it is plausible that these two signals correspond to distinct BN_3 environments.

Stability of BNH Polymers under Different Atmospheres

PAB and PB were stored for six months in the glovebox under three different atmospheres (argon, carbon dioxide, and oxygen) and at 25 °C to investigate their evolution over time using IR and ^{11}B MAS NMR spectroscopies (Figure S6). We discarded

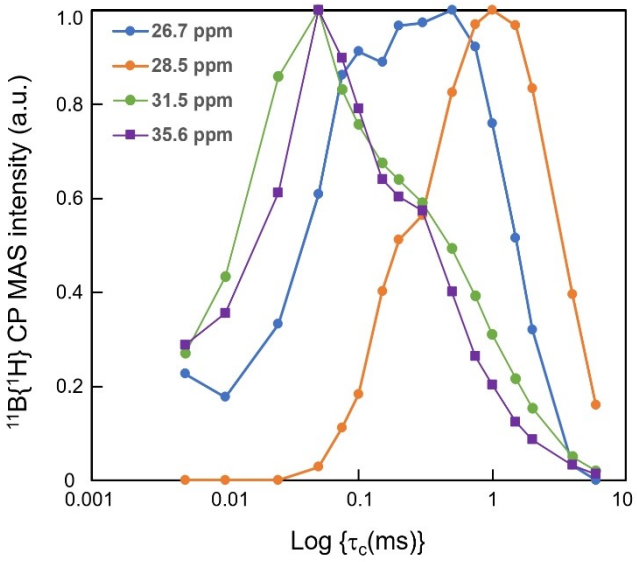

Figure 4. $^{11}B\{^1H\}$ CP MAS intensities (re-normalized) as a function of contact time τ_c for the four ^{11}B PB signals identified (Table 1). The log-scale is chosen for τ_c to better evidence the differences between CP dynamics.

ambient air because of the presence of moisture and the sensitivity of the polymers to hydrolysis in the presence of water molecules. The IR spectra of PAB exhibit no discernible changes regardless of the storage atmosphere. However, PAB stored under CO_2 displays an additional peak at about 1680 cm^{-1}, attributed to C═O bonds. This indicates that CO_2 molecules were adsorbed by PAB. This polymer contains a significant number of $–NH_2$ groups, which are well-known for their affinity for CO_2.[56] This finding implies that PAB could be of interest as a potential CO_2 adsorbent.

In contrast, the ^{11}B MAS NMR spectra reveal significant changes over time. The signals become broader, pointing out a higher degree of polymerization. The BH_4 signal persists after six months under all atmospheres, confirming that DADB remains stable over time. Notably, the two distinct NBH_3 signals initially observed in PAB have merged in a single signal, indicating that the transient phase of AB has evolved into PAB. For PAB stored under CO_2 and O_2, the signal around 0 ppm is more intense compared to the one stored under Ar. This observation implies that BO_4 environments are formed due to the interaction between O and B atoms in PAB.[57] These changes are not visible in the IR spectra, likely due to signal overlap in the region where B–O bonds typically appear in the 1300–1700 cm^{-1} region.[58] Additionally, the small signal observed at positive chemical shifts in PAB has increased in intensity and broadened, indicating a higher degree of cross-linking, as discussed in the next paragraph.

Similarly, the IR spectra of PB show no significant changes over time. The spectrum of PB stored under CO_2 also exhibits a small band at approximately 1680 cm^{-1}, attributed to adsorbed CO_2, though this band is less intense compared to that of PAB. The ^{11}B MAS NMR spectra of PB also show notable changes. Consistent with observations for PAB, the signal at negative chemical shifts broadens, suggesting increased polymerization. Furthermore, the signal at positive chemical shifts becomes broader and its shape evolves. This shape, indicative of a stronger quadrupolar effect, resembles that of boron nitride.[45,59] This suggests that PB has undergone further polymerization and likely achieved complete cross-linking. The spectra of PB stored under O_2 and CO_2 also exhibit a more intense band around 0 ppm compared to the sample stored under argon. This indicates that PB, like PAB, interacts with oxygen-containing gases to form BO_4 environments.

Overview of BNH Polymers

Based on the IR, XPS, and ^{11}B NMR results, it is evident that PAB is a mixture of compounds, primarily consisting of DADB and PAB along with PB. These findings indicate that obtaining a "pure" linear PAB under these conditions is challenging due to the simultaneous reactions that occur during the thermolysis of AB.[48] Additionally, even at relatively low temperatures such as 85 °C, the formation of PB cannot be avoided. Residual PAB is still detected in PB even after heating at 140 °C for 48 hours. PB is characterized by four distinct boron environments, two of which are in close proximity to protons. Based on these observations, a dehydrogenation scheme for AB under isothermal conditions is proposed (Scheme 1). This scheme considers that complex PAB (linear and branched, with NBH_3, N_2BH_2, N_3BH, and N_4B environments) formed alongside DADB, with PIB not being produced. The resulting PB exhibits a certain degree of cross-linking. The proposed dehydrogenation pathway also considers the different boron environments of PB, as identified by ^{11}B MQ MAS NMR. Two different BN_3, one located at the center of the hexagonal rings of PB, and the other at the edges connecting the cross-linked PAB with the end borazine-like chains. The two N_2BH environments are assigned to the B at the edges of the structure and the B in the borazine-like rings in the end chains.

In terms of stability, both PAB and PB undergo significant evolution over time. After 6 months of storage under various atmospheres, both polymers exhibited an increased degree of polymerization. In the presence of O_2 or CO_2, the BNH polymers formed borate-like compounds. Additionally, PAB demonstrated a capacity to adsorb some CO_2, highlighting a potential for CO_2 capture.

Regeneration Attempts of BNH Polymers

A critical step in utilizing AB for hydrogen storage is the development of a reversible system. However, the thermodynamically irreversible nature of the thermolysis reaction remains a significant challenge for this compound. In the pursuit of a simpler and more cost-effective regeneration method, we conducted experiments, never reported before to our knowledge, aimed at regenerating AB.

The initial set of experiments was inspired by processes in the hydrocracking industry, which effectively use platinum catalysts, heat and hydrogen pressure for producing small

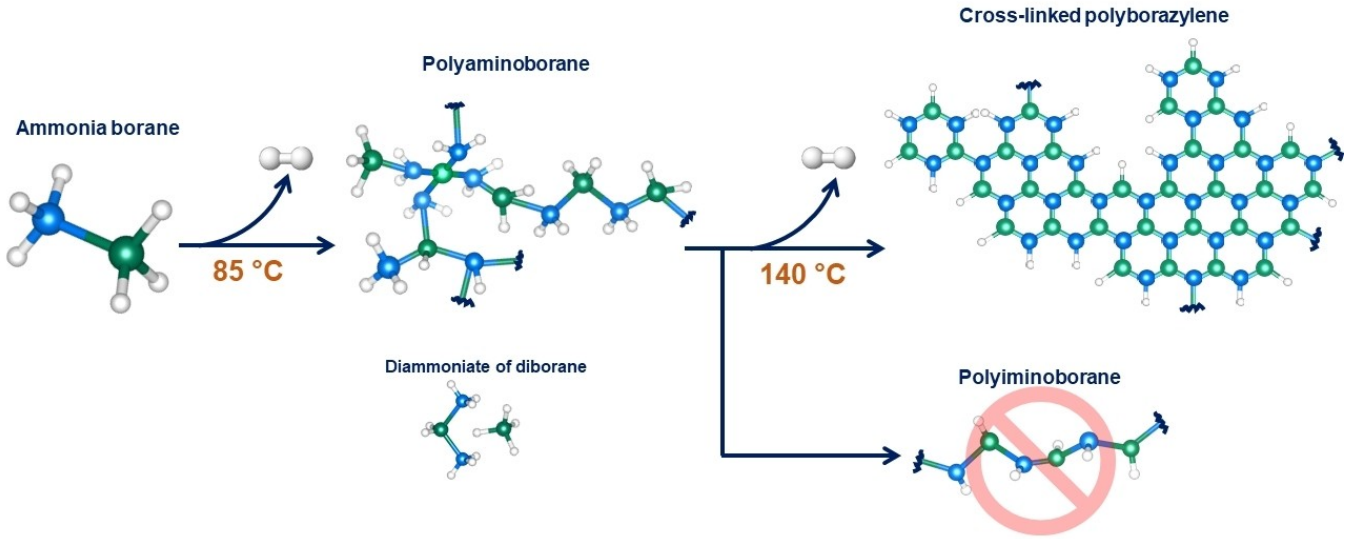

Scheme 1. Thermal dehydrogenation of ammonia borane under isothermal conditions. Ammonia borane releases the first equivalent of H_2 and it forms polyaminoborane (linear and branched presenting NBH_3, N_2BH_2, N_3BH, and N_4B environments, as detected by ^{11}B MAS NMR) and diammoniate of diborane. When this is heated at 140 °C, the second equivalent of H_2 is released and cross-linked polyborazylene is formed. The blue, green, and white spheres represent the nitrogen, boron, and hydrogen atoms, respectively.

alkanes and alkenes from heavier fractions. The goal was to break the BNH polymer chains in the presence of hydrogen to rehydrogenate the fragments and ideally convert them back into AB (or any other smaller hydrogenated fragments). The principle of this method is straightforward: regeneration reactions are performed on BNH polymers, which are insoluble in the chosen solvent (diglyme in this study), adding H_2 pressure and a mild temperature. If AB is formed during the process, it dissolves readily in diglyme and can be easily separated from the residual BNH solid polymer due to AB's high solubility in this solvent (0.27 g_{AB} $g^{-1}_{diglyme}$).[60] The resulting solution from these regeneration attempts was analyzed using ^{11}B NMR. Additional conditions were tested, including ultrasonication of the solid-state polymer under H_2 pressure and the use of NH_3 (as a Lewis base, it was expected to 'trap' any BH_3 species stemming from excessive fragmentation of PAB) in combination with H_2. Comprehensive experimental details, including conditions and outcomes, are provided in the Supporting Information and in Table S1. As shown in Figure 5a, PAB is insoluble in diglyme. Experiment 1 involved heating the PAB–diglyme suspension under stirring under mild conditions (65 °C) in an argon atmosphere for 24 h. Even under these conditions, PAB decomposed into smaller molecules. The ^{11}B NMR spectrum of Experiment 1 reveals six signals centered at 30.3, 24.7, −5.7, −11.5, −22.5, and −27.3 ppm. This suggests that PAB follows a thermolysis pathway similar to that of AB in a solvent.[61–63] Specifically, the signals at −22.5, −11.5, and −5.7 ppm are assigned to B-(cyclodiborazanyl)aminoborohydride (BCDB, Figure S7). It has been reported that the signal at −11.5 ppm contains contributions from BCDB, cyclotriborazane (CTB), and cyclodiborazane (CDB).[61] The signal at −27.3 ppm corresponds to aminodiborane (ADB), and the signals at positive chemical shifts at 30 and 25 ppm are attributed to borazine and polyborazylene, respectively.[62] Then, we performed Experiments 2 and 3. Experiment 2 was performed under 50 bar H_2 at 65 °C. With Experiment 3 we added a platinum catalyst. Experiments 2 and 3 yielded spectra similar to that of Experiment 1, indicating that the Pt catalyst is not really required in our experimental conditions to break down PAB. However, performing the reaction in a hydrogen atmosphere inhibited the formation of ADB. Increasing the reaction temperature to 80 °C or 120 °C favored the formation of borazine from PAB, as shown in the spectra of Experiments 4 and 6. When the reaction was carried out at 80 °C with a shorter reaction time of 6 hours (Experiment 5), the spectrum was similar to those of Experiments 2 and 3 (both lasting 24 h), indicating that temperatures above 80 °C are required to convert BCDB, CTB, and CDB into borazine. Experiment 7, conducted under a constant bubbling of hydrogen instead of a H_2 pressure, resulted in weak signals at −23 and −11.7 ppm, suggesting a similar reaction mechanism as in the pressurized reactor but to a lesser extent. PAB subjected to ultrasonication under hydrogen pressure (Experiment 8) showed no observable signals (Figure S8). Similarly, using

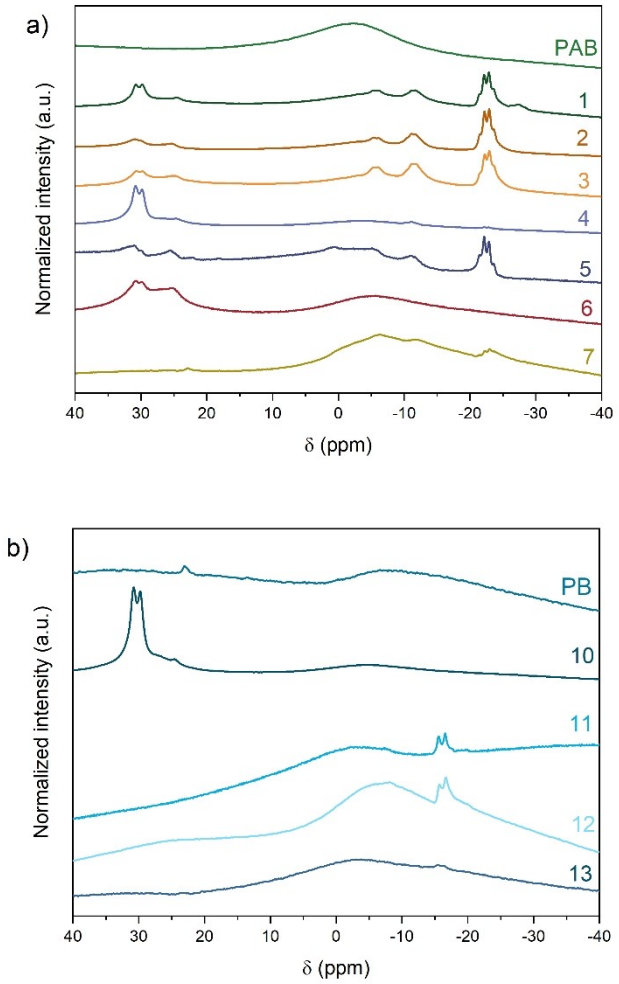

Figure 5. a) PAB; and b) PB ^{11}B NMR spectra of the experiments performed to regenerate these polymers. (See entries on Table S1).

ammonia and hydrogen pressure (Experiment 9) resulted in the formation of BCDB, CDB, and CTB (Figure S9).

In the case of PB, a small fraction of it is soluble in diglyme, as indicated by the low-intensity signal at 23 ppm in Figure 5b. This is likely attributable to the end chains of cross-linked PB. Regeneration experiments for PB differed from those for PAB. Heating PB at 120 °C under an argon atmosphere during 24 h led to the formation of borazine (Experiment 10). Experiments 11 to 13 were performed under H_2 pressure, then with a platinum catalyst, and finally under hydrogen bubbling. The spectra are similar to one another, though spectrum 13, obtained under a constant hydrogen bubbling, shows lower intensity. It is evident that hydrogen pressure alters the decomposition mechanism of PB, though, as with PAB, the use of our selected catalyst does not affect the reaction pathway. Notably, a new signal at −16 ppm was observed, which has not been reported in previous studies. This signal appears in the N_2BH_2 region of the ^{11}B NMR spectrum and may indicate that a fraction of PB underwent decomposition and partial rehydrogenation under hydrogen pressure. The experiment performed in an ultrasonic bath (Experiment 10) could not break the PB structure (Figure S10). The IR spectrum of PB subjected to ammonia and hydrogen pressure (Experiment 11) shows changes in the NH and BH stretching bands (Figure S11), suggesting partial rehydrogenation of the –NH and –BH groups in PB.

Overview of the Regeneration of BNH Polymers

For PAB, ^{11}B NMR analysis revealed that decomposition occurs even under mild conditions (i.e. 65 °C), leading to the formation of smaller compounds, including BCDB, CTB, CDB, ADB and borazine. The decomposition pathway appeared to mirror that of AB. Higher temperatures (above 80 °C) promoted the conversion of BCDB, CTB, and CDB into borazine. Interestingly, the use of hydrogen pressure suppressed ADB formation but did not alter the overall reaction pathway, nor was a catalyst required to facilitate decomposition. Experiments with ultrasonication and ammonia combined with hydrogen pressure were unsuccessful, with minimal observable rehydrogenation or molecular changes. In all the investigated conditions, PAB transforms in smaller compound. Although AB does not ultimately form, this is a first step towards the recycling of PAB. Future studies could explore two alternatives. The first one could be the full and selective decomposition of PAB into borazine, which is soluble in organic solvents, and has a high vapor pressure at 20–40 °C. These properties could be advantageous for, in a subsequent step, hydrocracking borazine in the gas phase and in the presence of a suitable, active heterogeneous catalyst. The second route is to explore effective and selective hydrogenation catalysts for borazine that would be active in the liquid phase. The ultimate objective would be to produce AB.

For PB, the regeneration process differed from PAB. Heating PB at 115 °C under an inert atmosphere resulted in the formation of borazine, while hydrogen pressure significantly modified the decomposition mechanism. A previously unreported signal in the ^{11}B NMR spectrum at −16 ppm, potentially indicative of partial rehydrogenation, was observed. However, the success of regeneration under these conditions was limited. The use of ammonia and hydrogen pressure caused partial rehydrogenation of the –NH and –BH groups in PB, as evidenced by changes in the IR spectrum, but the results were minor and far from complete regeneration. As for PAB, future studies should be oriented towards searching for active and selective catalysts towards the hydrogenation of PB.

Conclusions

In this study, we demonstrated that the thermolysis of AB under isothermal conditions leads to the formation of PAB and DADB, accompanied by the release of the first equivalent of H_2 at 85 °C. Further heating to 140 °C results in the formation of cross-linked PB. Notably, PIB was not identified, and it is unlikely to form under these conditions. Given the insolubility of these

BNH polymers, their characterization relies exclusively on solid-state techniques, including IR, Raman, XPS, and ^{11}B MAS NMR, which provide essential insights into their structural and chemical properties. These characterization methods underscored the structural complexity and chemical diversity of BNH polymers. They highlighted the challenges in achieving pure, linear PAB and in controlling the degree of polymerization and cross-linking in PB. This thorough understanding of BNH polymers provides a wider knowledge on their structure, to explore their potential applications in hydrogen storage and other fields (such as CO_2 adsorption).

The potential of AB as a hydrogen carrier relies heavily on the capability to regenerate its thermolysis products back into the borane. This research focused on addressing this challenge by exploring the regeneration of PAB and PB through experimental methods and pathways inspired by processes in the hydrocracking industry, which effectively use platinum catalysts, heat and hydrogen pressure. The results demonstrated that PAB and PB undergo decomposition and partial rehydrogenation under specific conditions, resulting in smaller molecules made of 2–3 nitrogen and boron atoms. This marks a step forward and could open the way for novel approaches to rehydrogenate BNH polymers formed during AB dehydrogenation. Thus, we believe that it is essential to further optimize reaction conditions, investigate effective hydrogenation heterogeneous catalysts, and develop strategies to address the inherent challenges associated with the thermodynamically irreversible pathways of AB decomposition.

Supporting Information

The experimental section and the information backing the results of this study can be found in the Supporting Information of this article.

Acknowledgements

This work was supported by funding from the French government, managed by the Agence Nationale pour la Recherche (ANR) as part of the France 2030 program, under the reference ANR-22-PEHY-0007 (SOLHYD project on solid-state hydrogen storage). The authors would like to express their gratitude to Christophe Charmette and Jim Cartier for their assistance with gas management during the regeneration experiments, to Eddy Petit for performing the Raman spectroscopy analyses, and to Emmanuel Fernandez for his help with the MAS NMR analyses.

Conflict of Interests

The authors declare no conflict of interest.

Data Availability Statement

Research data are not shared.

Keywords: ammonia borane · thermolysis · polyaminoborane · polyborazylene · regeneration

[1] L. Mulky, S. Srivastava, T. Lakshmi, E. R. Sandadi, S. Gour, N. A. Thomas, S. Shanmuga Priya, K. Sudhakar, *Mater. Chem. Phys.* **2024**, *325*, 129710.
[2] E. harrak Abdechafik, H. Ait Ousaleh, S. Mehmood, Y. Filali Baba, I. Bürger, M. Linder, A. Faik, *Int. J. Hydrogen Energy* **2024**, *52*, 1182–1193.
[3] R. Nagar, S. Srivastava, S. L. Hudson, S. L. Amaya, A. Tanna, M. Sharma, R. Achayalingam, S. Sonkaria, V. Khare, S. S. Srinivasan, *Sol. Compass* **2023**, *5*, 100033.
[4] J. Huo, K. Zhang, H. Wei, L. Fu, C. Zhao, C. He, X. Hu, *Chinese Chem. Lett.* **2023**, *34*, 108280.
[5] S. Frueh, R. Kellett, C. Mallery, T. Molter, W. S. Willis, C. King'Ondu, S. L. Suib, *Inorg. Chem.* **2011**, *50*, 783–792.
[6] F. Baitalow, J. Baumann, G. Wolf, K. Jaenicke-Rößler, G. Leitner, K. Jaenicke-Roößler, G. Leitner, *Thermochim. Acta* **2002**, *391*, 159–168.
[7] M. G. Hu, R. A. Geanangel, W. W. Wendlandt, *Thermochim. Acta* **1978**, *23*, 249–255.
[8] M. R. Weismiller, S. Q. Wang, A. Chowdhury, S. T. Thynell, R. A. Yetter, C *Thermochim. Acta* **2013**, *551*, 110–117.
[9] S. Bhunya, P. M. Zimmerman, A. Paul, *ACS Catal.* **2015**, *5*, 3478–3493.
[10] U. B. Demirci, S. Bernard, R. Chiriac, F. Toche, P. Miele, *J. Power Sources* **2011**, *196*, 279–286.
[11] D. J. Heldebrant, A. Karkamkar, N. J. Hess, M. Bowden, S. Rassat, F. Zheng, K. Rappe, T. Autrey, *Chem. Mater.* **2008**, *20*, 5332–5336.
[12] S. Hausdorf, F. Baitalow, G. Wolf, F. O. R. L. Mertens, *Int. J. Hydrogen Energy* **2008**, *33*, 608–614.
[13] B. L. Davis, D. A. Dixon, E. B. Garner, J. C. Gordon, M. H. Matus, B. Scott, F. H. Stephens, *Angew. Chemie* **2009**, *121*, 6944–6948.
[14] A. D. Sutton, A. K. Burrell, D. A. Dixon, E. B. Garner, J. C. Gordon, T. Nakagawa, K. C. Ott, J. P. Robinson, M. Vasiliu, *Science (80-.).* **2011**, *331*, 1426–1429.
[15] T. Q. Hua, R. K. Ahluwalia, *Int. J. Hydrogen Energy* **2012**, *37*, 14382–14392.
[16] N. Arulsamy, *J. Chem. Educ.* **2018**, *95*, 1381–1385.
[17] J. Li, S. M. Kathmann, H.-S. Hu, G. K. Schenter, T. Autrey, M. Gutowski, *Inorg. Chem.* **2010**, *49*, 7710–7720.
[18] E. R. Lory, R. F. Porter, *J. Am. Chem. Soc.* **1973**, *95*, 1766–1770.
[19] C. R. Miranda, G. Ceder, *J. Chem. Phys.* **2007**, *126*, 184703.
[20] H. M. Jeong, W. H. Shin, J. H. Park, J. H. Choi, J. K. Kang, *Nanoscale* **2014**, *6*, 6526–6530.
[21] T. Kobayashi, S. Gupta, M. A. Caporini, V. K. Pecharsky, M. Pruski, *J. Phys. Chem. C* **2014**, *118*, 19548–19555.
[22] O. Ayhan, T. Eckert, F. A. Plamper, H. Helten, *Angew. Chemie Int. Ed.* **2016**, *55*, 13321–13325.
[23] O. Ayhan, N. A. Riensch, C. Glasmacher, H. Helten, *Chem. – A Eur. J.* **2018**, *24*, 5883–5894.
[24] A. Paolone, F. Teocoli, S. Sanna, O. Palumbo, T. Autrey, *J. Phys. Chem. C* **2013**, *117*, 729–734.
[25] T. He, J. Wang, G. Wu, H. Kim, T. Proffen, A. Wu, W. Li, T. Liu, Z. Xiong, C. Wu, H. Chu, J. Guo, T. Autrey, T. Zhang, P. Chen, *Chem. – A Eur. J.* **2010**, *16*, 12814–12817.
[26] A. Staubitz, A. Presa Soto, I. Manners, *Angew. Chemie Int. Ed.* **2008**, *47*, 6212–6215.
[27] C. Zou, C. Zhang, B. Li, S. Wang, Z. Xie, Y. Song, *Mater. Sci. Eng. A* **2015**, *620*, 420–427.
[28] A. Liu, Y. Song, *J. Phys. Chem. C* **2012**, *116*, 2123–2131.
[29] R. Hinojosa-Nava, E. V. Mejía-Uriarte, A. R. Vázquez-Olmos, R. Y. Sato-Berrú, *Spectrochim. Acta - Part A Mol. Biomol. Spectrosc.* **2023**, *284*, DOI 10.1016/j.saa.2022.121776.
[30] S. F. Parker, *RSC Adv.* **2018**, *8*, 23875–23880.
[31] M. E. Bowden, G. J. Gainsford, W. T. Robinson, *Aust. J. Chem.* **2007**, *60*, 149–153.
[32] S. Gao, B. Li, D. Li, C. Zhang, R. Liu, S. Wang, *Ceram. Int.* **2018**, *44*, 11424–11430.
[33] A. V. Naumkin, A. Kraust-Vass, S. W. Gaarenstroom, C. J. Powell, NIST XPS Database, "NIST XPS Database," can be found under https://srdata.nist.gov/xps/Default.aspx, **2020**.

[34] P. Bachmann, F. Düll, F. Späth, U. Bauer, H. P. Steinrück, C. Papp, *J. Chem. Phys.* **2018**, *149*, DOI 10.1063/1.5051595.
[35] E. M. Freiberger, F. Düll, P. Bachmann, J. Steinhauer, F. J. Williams, H.-P. Steinrück, C. Papp, *J. Chem. Phys.* **2024**, *160*, DOI 10.1063/5.0202431.
[36] C. A. Castilla-Martinez, L. Roussignol, U. B. Demirci, *Int. J. Hydrogen Energy* **2021**, *46*, 33164–33175.
[37] P. J. Fazen, E. E. Remsen, J. S. Beck, P. J. Carroll, A. R. McGhie, L. G. Sneddon, *Chem. Mater.* **1995**, *7*, 1942–1956.
[38] M. Leboeuf, N. Russo, D. R. Salahub, M. Toscano, *J. Chem. Phys.* **1995**, *103*, 7408–7413.
[39] D. Jacquemin, E. A. Perpète, V. Wathelet, J.-M. André, *J. Phys. Chem. A* **2004**, *108*, 9616–9624.
[40] W. Harshbarger, G. H. Lee, R. F. Porter, S. H. Bauer, *Inorg. Chem.* **1969**, *8*, 1683–1689.
[41] S. Roy, X. Zhang, A. B. Puthirath, A. Meiyazhagan, S. Bhattacharyya, M. M. Rahman, G. Babu, S. Susarla, S. K. Saju, M. K. Tran, L. M. Sassi, M. A. S. R. Saadi, J. Lai, O. Sahin, S. M. Sajadi, B. Dharmarajan, D. Salpekar, N. Chakingal, A. Baburaj, X. Shuai, A. Adumbumkulath, K. A. Miller, J. M. Gayle, A. Ajnsztajn, T. Prasankumar, V. V. J. Harikrishnan, V. Ojha, H. Kannan, A. Z. Khater, Z. Zhu, S. A. Iyengar, P. A. da S Autreto, E. F. Oliveira, G. Gao, A. G. Birdwell, M. R. Neupane, T. G. Ivanov, J. Taha-Tijerina, R. M. Yadav, S. Arepalli, R. Vajtai, P. M. Ajayan, *Adv. Mater.* **2021**, *33*, 2101589.
[42] A. C. Stowe, W. J. Shaw, J. C. Linehan, B. Schmid, T. Autrey, *Phys. Chem. Chem. Phys.* **2007**, *9*, 1831–1836.
[43] M. Bowden, D. J. Heldebrant, A. Karkamkar, T. Proffen, G. K. Schenter, T. Autrey, *Chem. Commun.* **2010**, *46*, 8564–8566.
[44] Q. Zhao, J. Li, E. J. M. Hamilton, X. Chen, *J. Organomet. Chem.* **2015**, *798*, 24–29.
[45] C. Gervais, E. Framery, C. Duriez, J. Maquet, M. Vaultier, F. Babonneau, *J. Eur. Ceram. Soc.* **2005**, *25*, 129–135.
[46] K. Shimoda, K. Doi, T. Nakagawa, Y. Zhang, H. Miyaoka, T. Ichikawa, M. Tansho, T. Shimizu, A. K. Burrell, Y. Kojima, *J. Phys. Chem. C* **2012**, *116*, 5957–5964.
[47] W. J. Shaw, M. Bowden, A. Karkamkar, C. J. Howard, D. J. Heldebrant, N. J. Hess, J. C. Linehan, T. Autrey, *Energy Environ. Sci.* **2010**, *3*, 796.
[48] J. F. Petit, E. Dib, P. Gaveau, P. Miele, B. Alonso, U. B. Demirci, *ChemistrySelect* **2017**, *2*, 9396–9401.
[49] L. Li, Q. Gu, Z. Tang, X. Chen, Y. Tan, Q. Li, X. Yu, *J. Mater. Chem. A* **2013**, *1*, 12263–12269.
[50] B. Roy, U. Pal, A. Bishnoi, L. A. O'Dell, P. Sharma, *Chem. Commun.* **2021**, *57*, 1887–1890.
[51] B. Roy, A. Hajari, J. Manna, P. Sharma, *Dalt. Trans.* **2018**, *47*, 6570–6579.
[52] C. Gervais, J. Maquet, F. Babonneau, C. Duriez, E. Framery, M. Vaultier, P. Florian, D. Massiot, *Chem. Mater.* **2001**, *13*, 1700–1707.
[53] J. Li, S. Bernard, V. Salles, C. Gervais, P. Miele, J. Li, *Chem. Mater.* **2010**, *22*, 2010–2019.
[54] D.-P. Kim, K.-T. Moon, J.-G. Kho, J. Economy, C. Gervais, F. Babonneau, *Polym. Adv. Technol.* **1999**, *10*, 702–712.
[55] T. Kobayashi, I. Z. Hlova, N. K. Singh, V. K. Pecharsky, M. Pruski, *Inorg. Chem.* **2012**, *51*, 4108–4115.
[56] J. Hack, N. Maeda, D. M. Meier, *ACS Omega* **2022**, *7*, 39520–39530.
[57] M. R. Hansen, T. Vosegaard, H. J. Jakobsen, J. Skibsted, *J. Phys. Chem. A* **2004**, *108*, 586–594.
[58] C. Gautam, A. K. Yadav, A. K. Singh, *ISRN Ceram.* **2012**, *2012*, 1–17.
[59] R. W. Dorn, M. J. Ryan, T.-H. Kim, T. W. Goh, A. Venkatesh, P. M. Heintz, L. Zhou, W. Huang, A. J. Rossini, *Chem. Mater.* **2020**, *32*, 3109–3121.
[60] F. Mertens, G. Wolf, F. Baitalow, Ammonia borane and related compounds as hydrogen source materials, in *Handb. Hydrog. Storage*, Wiley, **2010**, pp. 215–247.
[61] W. J. Shaw, J. C. Linehan, N. K. Szymczak, D. J. Heldebrant, C. Yonker, D. M. Camaioni, R. T. Baker, T. Autrey, *Angew. Chemie - Int. Ed.* **2008**, *47*, 7493–7496.
[62] A. Al-Kukhun, H. T. Hwang, A. Varma, *Int. J. Hydrogen Energy* **2013**, *38*, 169–179.
[63] J. S. Wang, R. A. Geanangel, *Inorganica Chim. Acta* **1988**, *148*, 185–190.
[64] J. Hannauer, U. B. Demirci, C. Geantet, J.-M. Herrmann, P. Miele, *Int. J. Hydrogen Energy* **2012**, *37*, 10758–10767.
[65] A. Medek, J. S. Harwood, L. Frydman, *J. Am. Chem. Soc.* **1995**, *117*, 12779–12787.
[66] J.-P. Amoureux, C. Fernandez, S. Steuernagel, *J. Magn. Reson. Ser. A* **1996**, *123*, 116–118.
[67] D. Massiot, *J. Magn. Reson. Ser. A* **1996**, *122*, 240–244.
[68] D. Massiot. "NMR@CEMHTI. Dmfit program". Can be found under https://nmr.cemhti.cnrs-orleans.fr/dmfit/. Last accessed on January 24th, 2025.
[69] D. Massiot, F. Fayon, M. Capron, I. King, S. Le Calvé, B. Alonso, J. Durand, B. Bujoli, Z. Gan, G. Hoatson, *Magn. Reson. Chem.* **2002**, *40*, 70–76.

Manuscript received: January 29, 2025
Revised manuscript received: February 20, 2025
Accepted manuscript online: February 28, 2025
Version of record online: March 12, 2025